

177914: leucocratic monzogranite, Kiaki Soak

Location and sampling

WIDGIEMOOLTHA (SH 51-14), MOUNT BELCHES (3335)
MGA Zone 51, 424022E 6541550N

Sampled on 3 May 2004

The sample was taken from a 2 m-diameter, partly buried boulder on the southern shore of Lake Randell, 14 km south of Kiaki Soak.

Tectonic unit/relations

The unit sampled is an inequigranular, leucocratic phase of the Kiaki Monzogranite, which forms the central part of the Randall Dome (Painter and Groenewald, 2001) within the Bulong Domain of the Kurnalpi Terrane, Eastern Goldfields Superterrane, Yilgarn Craton (Cassidy et al., 2006). Along the margin of the Randall Dome, about 15 km to the north, granitic rocks appear to intrude (and hornfels) complexly-deformed rocks of the Mount Belches Formation (Painter and Groenewald, 2001), which have a maximum depositional age of 2660 ± 14 Ma (GSWA 177915; Wingate and Bodorkos, 2007).

Petrographic description

The visually estimated primary mineralogy of this sample comprises 40–45% quartz, 35% plagioclase, 20% microcline, 2% hornblende, and 1% titanite. Quartz forms undeformed interstitial grains to 7 mm in association with inequigranular aggregates of plagioclase and microcline, comprising grains 0.2–3 mm in size. Small grains of green hornblende (up to 1.5 mm) and titanite (less than 1 mm) are disseminated, as well as rare apatite and zircon crystals about 50 μ m long.

Lower greenschist facies metamorphism is indicated by the development of minor epidote within plagioclase, and in association with biotite adjacent to hornblende. Biotite in turn has largely been replaced by chlorite. Irregular clay patches in feldspars probably reflect incipient weathering.

Zircon morphology

The zircons isolated from this sample are subhedral to euhedral, and mainly clear and colourless. They are up to 350 μ m long, with aspect ratios up to 4:1. Concentric growth zoning is ubiquitous, and several

zircons show disrupted internal structures, consistent with alteration. Most zircons are strongly cracked. Most possess high-uranium outer growth zones that are dark in cathodoluminescence images. Cathodoluminescence images of representative zircons are shown in Figure 1.

Analytical details

This sample was analysed on 16 January 2005 (using SHRIMP-B) and 17 January 2005 (using SHRIMP-A). Analyses 1.1 to 16.1 (spot numbers 1–16 inclusive) were obtained during the first session, together with 12 analyses of the CZ3 standard that indicated an external spot-to-spot (reproducibility) uncertainty of 1.00% (1σ), and a $^{238}\text{U}/^{206}\text{Pb}^*$ calibration uncertainty of 0.36% (1σ). Analyses 17.1 to 24.2 (spot numbers 17–29 inclusive) were obtained during the second session, together with nine analyses of the CZ3 standard that indicated an external spot-to-spot (reproducibility) uncertainty of 2.30% (1σ), and a $^{238}\text{U}/^{206}\text{Pb}^*$ calibration uncertainty of 0.89% (1σ). Calibration uncertainties are included in the errors of $^{238}\text{U}/^{206}\text{Pb}^*$ ratios and dates quoted in Table 1. Common-Pb corrections were applied to all analyses using contemporaneous common Pb isotopic compositions determined by the method of Stacey and Kramers (1975).

Results

Twenty-nine analyses were obtained from 26 zircons, with three grains (13, 15, and 24) each analysed twice. Results are listed in Table 1, and shown in a concordia diagram (Fig. 2).

Interpretation

The analyses range from concordant to strongly discordant, and the pattern of discordance is consistent with episodes of both ancient and recent loss of radiogenic Pb from some zircons (Fig. 2). Two analyses (6.1 and 7.1) were significantly affected by instability in the primary beam during analysis, and a further 11 analyses, mostly of zircon rims with high uranium contents, are characterized by moderate to strong discordance ($>10\%$), or high common-Pb contents ($f_{204} > 2\%$). The dates obtained from all 13 of these analyses (Group D; Table 1) are imprecise or unreliable, and are not considered geologically significant. The remaining 16 analyses can be divided into two groups, based on their $^{207}\text{Pb}^*/^{206}\text{Pb}^*$ and Th/U ratios.

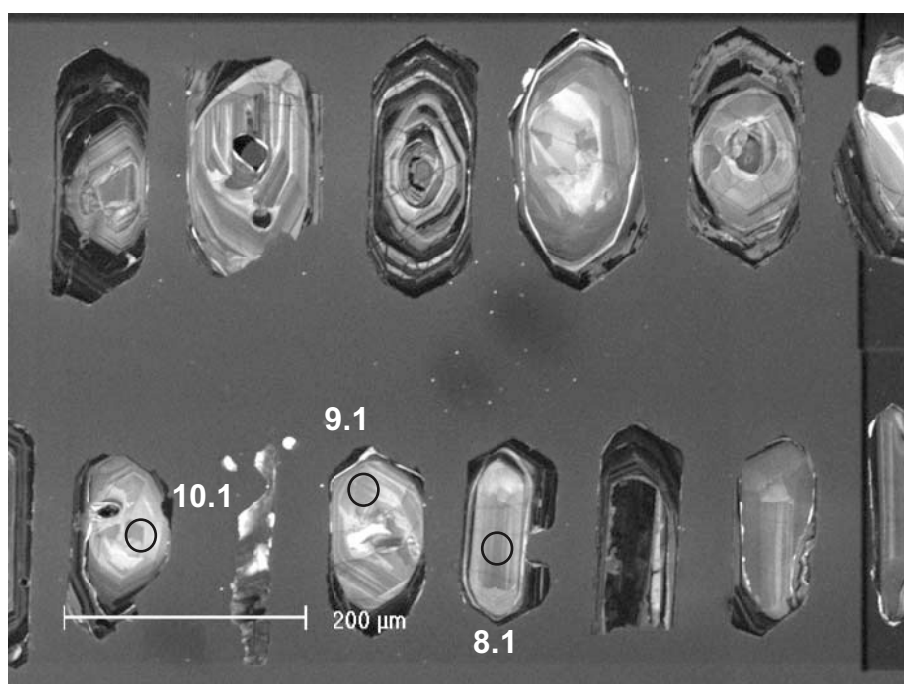


Figure 1. Cathodoluminescence image of representative zircons from sample 177914: leucocratic monzogranite, Kiaki Soak. Numbered circles indicate approximate positions of analysis sites

Group 1 comprises 15 analyses of 14 zircons (Table 1) with moderate to high Th/U (0.37–1.48), which yield a weighted mean $^{207}\text{Pb}^*/^{206}\text{Pb}^*$ date of 2692 ± 8 Ma (MSWD = 0.72).

Group 2 comprises a single analysis (Table 1) with low Th/U (0.10), which yields a $^{207}\text{Pb}^*/^{206}\text{Pb}^*$ date of 2666 ± 6 Ma (1σ).

The geological significance of the dates obtained from Groups 1 and 2 is unclear, and two interpretations are possible. The first of these is the preferred interpretation, but the second cannot be precluded on the basis of these results.

If the Kiaki Monzogranite is coeval with the granitic rocks responsible for contact metamorphism of the c. 2660 Ma Mount Belches Formation (GSWA 177915; Wingate and Bodorkos, 2007) in the northern Randall Dome, then the date of 2692 ± 8 Ma for the 15 analyses in Group 1 probably represents the age of a dominant xenocrystic zircon component in the source region of the Kiaki Monzogranite. In this scenario, the date of 2666 ± 6 Ma (1σ) for the single analysis (26.1) in Group 2 could represent zircon growth during igneous crystallization, and it is possible that the high-uranium rims also formed during igneous crystallization, although this cannot be demonstrated from the highly discordant results (Fig. 2).

Alternatively, if the Kiaki Monzogranite is not coeval with the granitic rocks that hornfelsed the Mount Belches Formation, then the date of 2692 ± 8 Ma for the 15

analyses in Group 1 may represent the age of igneous crystallization of the Kiaki Monzogranite. In this scenario, the Kiaki Monzogranite represents an older (basement) component of a composite granitic intrusion in the Randall Dome, and contact metamorphism of the Mount Belches Formation reflects emplacement of granitic material significantly younger than the Kiaki Monzogranite. The date of 2666 ± 6 Ma (1σ) for the single analysis (26.1) in Group 2 could represent zircon growth with the Kiaki Monzogranite during this contact metamorphic event, and it is possible that the high-uranium rims also formed during metamorphism, although this cannot be demonstrated from the highly discordant results (Fig. 2).

References

- CASSIDY, K. F., CHAMPION, D. C., KRAPEŽ, B., BARLEY, M. E., BROWN, S. J. A., BLEWETT, R. S., GROENEWALD, P. B., and TYLER, I. M., 2006, A revised geological framework for the Yilgarn Craton, Western Australia: Western Australia Geological Survey, Record 2006/8, 8p.
- PAINTER, M. G. M., and GROENEWALD, P. B., 2001, Geology of the Mount Belches 1:100 000 sheet: Western Australia Geological Survey, 1:100 000 Geological Series Explanatory Notes, 38p.
- STACEY, J. S., and KRAMERS, J. D., 1975, Approximation of terrestrial lead isotope evolution by a two-stage model: *Earth and Planetary Science Letters*, v. 26, p. 207–221.
- WINGATE, M. T. D., and BODORKOS, S., 2007, 177915: metasandstone, Randalls Mine; Geochronology dataset 664, in *Compilation of geochronology data: Western Australia Geological Survey*.

Table 1. Ion microprobe analytical results for zircons from sample 177914: leucocratic monzogranite, Kiaki Soak

Grp no.	Spot no.	Grain .spot	^{238}U (ppm)	^{232}Th (ppm)	$\frac{^{232}\text{Th}}{^{238}\text{U}}$	f_{204} (%)	$^{238}\text{U}/^{206}\text{Pb}$ $\pm 1\sigma$	$^{207}\text{Pb}/^{206}\text{Pb}$ $\pm 1\sigma$	$^{238}\text{U}/^{206}\text{Pb}^*$ $\pm 1\sigma$	$^{207}\text{Pb}^*/^{206}\text{Pb}^*$ $\pm 1\sigma$	$^{238}\text{U}/^{206}\text{Pb}^*$ date (Ma) $\pm 1\sigma$	$^{207}\text{Pb}^*/^{206}\text{Pb}^*$ date (Ma) $\pm 1\sigma$	Disc (%)
1	9	9.1	74	57	0.80	0.064	1.958 \pm 0.036	0.18830 \pm 0.00174	1.959 \pm 0.036	0.18773 \pm 0.00195	2658 \pm 40	2722 \pm 17	2.3
1	16	16.1	44	30	0.71	-0.283	1.976 \pm 0.038	0.18480 \pm 0.00294	1.970 \pm 0.038	0.18733 \pm 0.00293	2646 \pm 41	2719 \pm 26	2.7
1	2	2.1	47	33	0.72	0.525	1.988 \pm 0.036	0.19058 \pm 0.00208	1.999 \pm 0.036	0.18590 \pm 0.00242	2615 \pm 39	2706 \pm 21	3.4
1	10	10.1	76	69	0.94	0.007	1.950 \pm 0.030	0.18488 \pm 0.00167	1.950 \pm 0.030	0.18481 \pm 0.00180	2669 \pm 34	2697 \pm 16	1.0
1	21	15.2	146	56	0.40	0.570	2.014 \pm 0.051	0.18972 \pm 0.00081	2.026 \pm 0.051	0.18464 \pm 0.00108	2586 \pm 54	2695 \pm 10	4.0
1	5	5.1	121	174	1.48	0.056	2.082 \pm 0.029	0.18511 \pm 0.00155	2.083 \pm 0.029	0.18461 \pm 0.00161	2528 \pm 30	2695 \pm 14	6.2
1	4	4.1	109	91	0.86	0.109	1.957 \pm 0.028	0.18534 \pm 0.00144	1.959 \pm 0.028	0.18438 \pm 0.00169	2658 \pm 31	2693 \pm 15	1.3
1	12	12.1	176	63	0.37	0.464	2.011 \pm 0.027	0.18842 \pm 0.00111	2.021 \pm 0.027	0.18428 \pm 0.00146	2592 \pm 28	2692 \pm 13	3.7
1	1	1.1	158	111	0.72	0.322	2.005 \pm 0.027	0.18709 \pm 0.00149	2.011 \pm 0.027	0.18422 \pm 0.00164	2602 \pm 29	2691 \pm 15	3.3
1	3	3.1	125	92	0.76	0.442	2.042 \pm 0.029	0.18806 \pm 0.00130	2.052 \pm 0.029	0.18412 \pm 0.00171	2560 \pm 31	2690 \pm 15	4.9
1	8	8.1	103	102	1.02	-0.059	1.962 \pm 0.028	0.18303 \pm 0.00135	1.961 \pm 0.028	0.18355 \pm 0.00138	2656 \pm 30	2685 \pm 12	1.1
1	11	11.1	153	134	0.91	0.786	2.077 \pm 0.035	0.18999 \pm 0.00122	2.094 \pm 0.036	0.18298 \pm 0.00197	2517 \pm 35	2680 \pm 18	6.1
1	15	15.1	52	35	0.69	0.316	1.949 \pm 0.035	0.18486 \pm 0.00204	1.956 \pm 0.036	0.18204 \pm 0.00306	2662 \pm 40	2672 \pm 28	0.3
1	13	13.1	74	41	0.57	0.057	2.006 \pm 0.032	0.18209 \pm 0.00164	2.007 \pm 0.032	0.18158 \pm 0.00182	2606 \pm 34	2667 \pm 17	2.3
1	14	14.1	63	28	0.46	0.195	1.998 \pm 0.055	0.18300 \pm 0.00220	2.002 \pm 0.055	0.18126 \pm 0.00242	2611 \pm 59	2664 \pm 22	2.0
2	28	26.1	191	18	0.10	0.045	1.893 \pm 0.049	0.18188 \pm 0.00068	1.894 \pm 0.049	0.18148 \pm 0.00069	2733 \pm 57	2666 \pm 6	-2.5
D	6	6.1	66	73	1.13	0.344	2.016 \pm 0.041	0.19908 \pm 0.01200	2.023 \pm 0.043	0.19602 \pm 0.01288	2589 \pm 45	2793 \pm 108	7.3
D	7	7.1	163	92	0.58	0.441	2.055 \pm 0.036	0.20306 \pm 0.01341	2.064 \pm 0.036	0.19913 \pm 0.01357	2547 \pm 37	2819 \pm 111	9.7
D	22	20.1	481	44	0.09	2.392	2.514 \pm 0.062	0.18364 \pm 0.00087	2.576 \pm 0.064	0.16233 \pm 0.00196	2115 \pm 45	2480 \pm 20	14.7
D	24	22.1	197	116	0.61	3.770	2.460 \pm 0.062	0.20875 \pm 0.00204	2.556 \pm 0.065	0.17514 \pm 0.00429	2129 \pm 46	2607 \pm 41	18.4
D	17	17.1	278	60	0.22	7.308	2.422 \pm 0.061	0.24650 \pm 0.00147	2.613 \pm 0.067	0.18138 \pm 0.00613	2089 \pm 46	2666 \pm 56	21.6
D	27	25.1	408	200	0.51	3.019	2.894 \pm 0.073	0.19200 \pm 0.00111	2.984 \pm 0.075	0.16510 \pm 0.00269	1863 \pm 41	2509 \pm 27	25.7
D	25	23.1	265	147	0.57	6.368	2.811 \pm 0.073	0.23574 \pm 0.00082	3.002 \pm 0.080	0.17898 \pm 0.00490	1853 \pm 43	2643 \pm 45	29.9
D	26	24.1	1167	159	0.14	3.973	4.911 \pm 0.122	0.13908 \pm 0.00186	5.114 \pm 0.128	0.10459 \pm 0.00357	1151 \pm 26	1707 \pm 63	32.6
D	29	24.2	384	180	0.48	9.634	2.986 \pm 0.074	0.25917 \pm 0.00080	3.304 \pm 0.086	0.17337 \pm 0.00745	1704 \pm 39	2590 \pm 72	34.2
D	19	18.1	456	100	0.23	15.969	3.619 \pm 0.090	0.31226 \pm 0.00138	4.307 \pm 0.123	0.17023 \pm 0.01294	1346 \pm 35	2560 \pm 127	47.4
D	20	19.1	591	204	0.36	19.463	4.068 \pm 0.101	0.31746 \pm 0.00101	5.052 \pm 0.152	0.14520 \pm 0.01546	1164 \pm 32	2290 \pm 183	49.2
D	18	13.2	325	149	0.47	7.661	4.163 \pm 0.110	0.23862 \pm 0.00350	4.509 \pm 0.123	0.17037 \pm 0.00742	1291 \pm 32	2561 \pm 73	49.6
D	23	21.1	531	495	0.96	21.241	4.700 \pm 0.118	0.35254 \pm 0.00121	5.968 \pm 0.190	0.16394 \pm 0.01780	999 \pm 29	2497 \pm 183	60.0

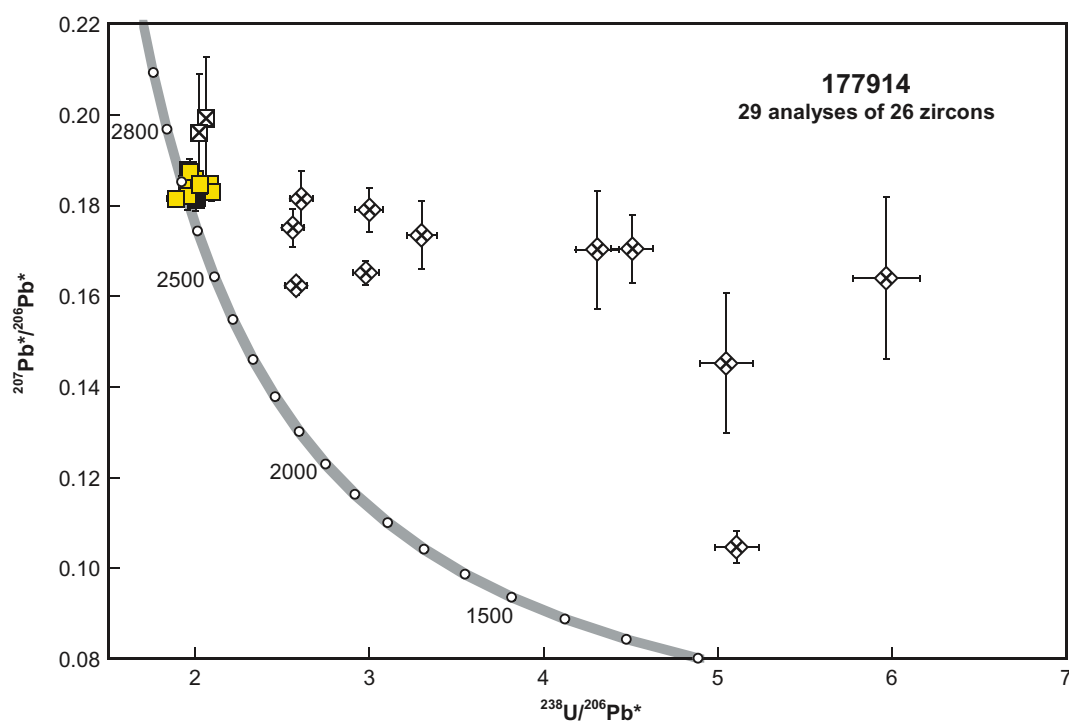


Figure 2. U–Pb analytical data for sample 177914: leucocratic monzogranite, Kiaki Soak. Yellow squares indicate Group 1 (xenocrystic zircon cores, or igneous crystallization); black square indicates Group 2 (igneous crystallization, or metamorphic zircon); crossed squares indicate ungrouped analyses (primary beam instability); crossed diamonds indicate ungrouped analyses (discordance >10% or f_{204} >2%)

Recommended reference for this publication

WINGATE, M. T. D., and BODORKOS, S., 2007, 177914: leucocratic monzogranite, Kiaki Soak; Geochronology dataset 663, in *Compilation of geochronology data: Western Australia Geological Survey*.

Data obtained: 17 January 2005
Data released: 31 May 2007